

Detecting cracks in teeth and monitoring structural integrity over time with non-invasive PTR-LUM technology a solution for a major clinical challenge

Cite as: J. Appl. Phys. **131**, 164501 (2022); <https://doi.org/10.1063/5.0088073>

Submitted: 12 February 2022 • Accepted: 07 April 2022 • Published Online: 25 April 2022

 Stephen H. Abrams and  Koneswaran S. Sivagurunathan



View Online



Export Citation



CrossMark

Lock-in Amplifiers
up to 600 MHz



Zurich
Instruments



Detecting cracks in teeth and monitoring structural integrity over time with non-invasive PTR-LUM technology a solution for a major clinical challenge

Cite as: J. Appl. Phys. **131**, 164501 (2022); doi: [10.1063/5.0088073](https://doi.org/10.1063/5.0088073)

Submitted: 12 February 2022 · Accepted: 7 April 2022 ·

Published Online: 25 April 2022



View Online



Export Citation



CrossMark

Stephen H. Abrams^{1,2,a)}  and Koneswaran S. Sivagurunathan^{2,3,4} 

AFFILIATIONS

¹Cliffcrest Dental Office, Toronto, Ontario M1M1P1, Canada

²Quantum Dental Technologies, Toronto, Ontario M6B1L3, Canada

³Center for Advanced Diffusion-Wave and Photoacoustic Technologies (CADIPT),

Department of Mechanical and Industrial Engineering, University of Toronto, Toronto, Ontario, Canada

⁴Institute for Advanced Non-Destructive and Non-Invasive Diagnostic Technologies (IANDIT), University of Toronto, Toronto, Ontario, Canada

Note: This paper is part of the Special Topic on Non-Invasive and Non-Destructive Methods and Applications Part I – Festschrift.

a) Author to whom correspondence should be addressed: dr.abrams4cell@sympatico.ca

ABSTRACT

Detecting cracks in teeth is a long-standing clinical challenge. Patients may complain of diffuse pain on chewing, pain, at times, on temperature change and pain that occurs episodically. Common diagnostic tools such as radiographs and visual examination may not detect cracks. This clinical case study shows how photothermal radiometry and luminescence (PTR-LUM), technology behind the Canary Dental Caries Detection System can detect and monitor cracks clinically as well as quantify the extent of crack. This important clinical feature is not yet available with other caries detection clinical devices. In this clinical situation, the cracks involved a large part of the mesial and distal of a mandibular second molar and the adjacent first molar. It led to a diagnosis of parafunction and placement of a mandibular flat plane bite splint along with the placement of composite restorations to restore the fractures. The science behind the point scan lock-in signal processing results of PTR-LUM technology implemented in The Canary System to clinically detect visible cracks or cracks beneath the enamel surface as well as caries on all tooth surfaces and around restorations is discussed. Amplitude and phase results from PTR-LUM point scans are incorporated into a Canary number output developed for oral health providers and are disclosed for the first time in detail with clinical evidence.

Published under an exclusive license by AIP Publishing. <https://doi.org/10.1063/5.0088073>

I. INTRODUCTION

Detecting cracks in teeth is one of the more challenging clinical situations. The “cracked tooth syndrome” was described over 55 years ago,¹ and clinicians still struggle to detect cracks early and to provide appropriate therapy.² Patients usually present with vague symptoms such as acute pain on mastication of grainy tough foods and sharp brief pain on cold. These findings relate to cusp fracture but there can also be other symptoms associated with a crack or fracture such as slight to severe pain consistent with irreversible pulpitis or pulpal necrosis.³ Periapical and bitewing radiographs

usually cannot image the crack or fracture. So, the dilemma is how does one detect and then manage cracks and fractures in teeth?

What are the predisposing factors to cracked teeth? A number of papers indicate that cracked teeth were associated with intra-coronal restorations and frequently found in mandibular molars.⁴⁻⁷ The most commonly identified etiologic factor was the design of the cavity preparations. Large restorations, inappropriate use of pins, restorations encroaching upon the marginal ridges, or undermining the marginal ridges are some of the factors. Selection of restorative materials may also be a factor. Bonded restorations may

possibly reduce the incidence of cracks or fractures. Bruxism and other parafunctional habits, wear, malocclusion, steep cuspal inclines, or deep occlusal grooves were also considered as predisposing factors.^{8–11} Cracks can also occur in intact teeth with no restorations. One study found that 28% of the longitudinal fractures occurred in teeth with no restorations,¹² while another study of 154 cases found that 60.4% had no restorations, and a further 29% had only class I restorations.¹³

COVID-19 has also had an impact on cracked teeth. The American Dental Association's Health Policy Institute latest data from their tracking poll conducted the week of February 15, 2021¹⁴ found that the vast majority of dentists indicate that the prevalence of stress-related oral health conditions among their respective patients have increased since the onset of the COVID-19 pandemic. More than 70% of dentists surveyed saw an increase in patients experiencing teeth grinding and clenching, conditions often associated with stress up from just fewer than 60% in the fall. More specifically, 71% of dentists surveyed reported an increase in the prevalence of teeth grinding and clenching; 63% for chipped teeth; 63% for cracked teeth; and 62% for temporomandibular joint disorder (TMD) symptoms, which includes headaches and jaw pain.¹⁴ A clinical online study done on populations in Israel and Poland in April and May 2020 found that "the Coronavirus pandemic had caused significant adverse effects on the psycho-emotional status of both Israeli and Polish populations, resulting in the intensification of their bruxism and TMD symptoms."¹⁵ Temporomandibular Disorders and bruxism are common causes for cracked teeth so early detection of cracks will also lead to treatment of TMD.

The clinical challenge is how to detect cracks in teeth? Patients may present complaining of pain on chewing but not consistently. The pain would only occur when loading teeth in a certain position. There may be pain on temperature change or this may not be a feature. Clinically, the teeth may look intact.² The marginal ridges may appear stained, but there are no grooves or cracks. Radiographs may not show any interproximal defects or caries.

In this clinical case report, we used The Canary System as one of the caries detection diagnostic tools for detecting cracks. The Canary System is a laser-based and point scan caries detection system that uses energy conversion technology called PTR-LUM, with an intra-oral camera to image and examine teeth.^{17,18} This case study found that The Canary System could also detect cracks in teeth, which were not always seen visually or with a radiograph.

II. MATERIALS AND METHOD

A. Clinical data collection with The Canary System

The Canary System directly assesses the status of the enamel crystal by using PTR-LUM technology. Pulses of laser light (660 nm wavelength) with 0.05 mm diameter of beam spot and about 40 mW laser power are shone on the enamel surface of a tooth for 5 s. The laser light is converted to heat (photothermal radiometry or PTR) and light (luminescence or LUM), which are emitted from the tooth surface. PTR signal is measured with an infrared detector (3–5 μm detectivity range) and LUM signal is measured with a photodiode (LUM after passing through a 710 nm cutoff filter). These harmless pulses of laser light allow one to

examine up to 5 mm below the tooth surface depending on the clinical situation of the probing surface.^{17,18} Carious lesions or defects on the enamel crystal structures modify the thermal properties (PTR) and glow (LUM) from the healthy teeth. As a lesion or defect grows, there is a corresponding change in the response signal as the heat is confined to the region with crystalline disintegration (dental caries or defects) and PTR strongly increases, while LUM weakly decreases in The Canary System. (LUM contribution is active on healthy tooth surfaces. Even though LUM contribution is set to be constant when PTR signal is detected in The Canary System, LUM contribution is critical to validate the stability of each Canary point scan result as well as to validate thin biofilm layers on enamel surfaces or not.) As remineralization progresses and enamel prisms begin to re-form their structure, the thermal and luminescence properties begin to revert back in the direction of healthy teeth. The PTR signal detector in The Canary System is sensitive enough to identify early defects in enamel crystal structures, as it detects very small changes in temperature (less than 1–2 $^{\circ}\text{C}$ ¹⁹), much less than that generated by a conventional dental curing light and imperceptible to the patient. Two Health Canada approved clinical trials have confirmed the safety and efficacy of The Canary System.^{17,18}

B. Physical foundations of the PTR-LUM technology

PTR LUM technology used in The Canary System is based on frequency-domain infrared photothermal radiometry (FD-PTR) and modulated laser luminescence as complementary dynamic dental diagnostic tools for quantifying sound and defective cracked enamel. Previous lab-based, proof of concept experimental and related theoretical work^{21–26} showed the complementarity between modulated luminescence and photothermal at fixed or frequency scans and investigated the sensitivity and spatial resolution of the PTR-LUM methodology applied to dental tissues, cracked, and sound enamel samples. The significance of previous studies heightened the potential of this technique to monitor small caries lesions, which initially started beneath the enamel surface, and the lesion size and depth were similar to cracks.

FD-PTR technique is based on the modulated thermal infrared blackbody or Planck-radiation response of a medium, resulting from radiation absorption, nonradiative energy conversion, and excited-to-ground-state relaxation, followed by temperature rise. The generated signals carry subsurface information in the form of a temperature depth integral. As a result, PTR has the ability to penetrate and yield information about an opaque medium well below the range of optical imaging. FD-PTR, exhibits much higher SNR and a fixed probe depth with the use of a single modulation frequency. A temperature oscillation due to modulated heating causes a variation in the thermal emissions, which is monitored using an infrared detector. The temperature modulation allows for thermal energy to reach the surface diffusively from a depth approximately equal to a thermal wavelength (λ) such that $\lambda(f) = \sqrt{\frac{4\pi\alpha}{f}}$, where α is the material thermal diffusivity (cm^2/s) and f is the laser-beam modulation frequency. Scatterers located within a fraction of a thermal wavelength from the source dominate the contrast of radiometric images. In this way, when the thermal wavelength is varied, e.g., by changing

the laser-beam modulation frequency, the region of the specimen that contributes to the image is also varied.²²

In this report, clinical validation of PTR-LUM technology is investigated with a commercially available dental caries detections device; The Canary System. The laser in the hand piece of The Canary System sends pulses of laser light onto a tooth surface. A fraction of the laser light is reflected, scattered, or transmitted from the tooth, and a part may be absorbed within the tooth. Scattering refers to the process whereby a photon interacts with small particles within the tooth, thereby changing its path without losing its energy. On the other hand, following absorption of the laser light, atoms or molecules within the tooth are raised from the ground state to excited higher-energy states. Excited atoms or molecules are unstable and de-excite to more stable lower-energy states. During de-excitation processes, the absorbed energy is converted to heat (PTR) or lower-energy light (LUM) that is then emitted back from the tooth (Fig. 1).

Laser is modulated at 2 Hz. Each Canary scan takes 6 s to complete and first second results are skipped for system stability, and the remaining 5 s results are used for the computation of the PTR-LUM amplitude and phase results. Hence, 10 cycles of PTR-LUM response signals are available from each Canary scan. PTR-LUM responses are also acquired with 51 200 sampling frequency so that each amplitude and phase calculations are carried out from $51\,200 \times 5 = 256\,000$ data points for each PTR and LUM channels from each Canary scan data. Infrared and photodiode detectors in the headpiece collect both the amplitude and phase output results which are computed by the software lock-in signal processing algorithm from PTR and LUM responses. Amplitude is the magnitude of the emitted heat and or light signals, while the phase is the time delay from the absorption of laser light by the tooth to the collection of the emitted heat and or light by the detectors. Therefore, The Canary System collects four sets of output data (amplitude and phase signals of both PTR and LUM responses) from the tooth surface. These output data are then used to calculate The Canary Number (17, 27).

C. Canary Number and Canary Scale

In order to explain the clinical findings of lesions and defects in the enamel crystal structure, the derivation of The Canary

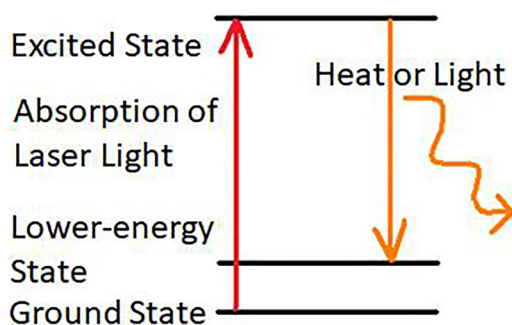


FIG. 1. Conversion of absorbed laser light to other forms of energy (heat or light) emitted back from tooth.

Number from PTR, LUM amplitude and phase are described in this section. The Canary System measures four signals:

- (1) The strength or amplitude of the converted heat (PTR).
- (2) The time delay or phase of the converted heat (PTR) to reach the surface.
- (3) The strength or amplitude of the emitted luminescence (LUM).
- (4) The time delay or phase of the emitted luminescence (LUM).

The Canary Number is created from an algorithm combining these four signals and is directly linked to the status of the enamel or root surface crystal structure,

$$\text{Canary Number (raw)} = C \left(\frac{\text{PTR Amp} \times \text{PTR Phase}}{\text{LUM Amp} \times \text{LUM Phase}} \right), \quad (1)$$

where PTR Amp = PTR amplitude; PTR phase = PTR phase; LUM amp = luminescence amplitude; LUM phase = luminescence phase; and C: instrumental normalization constant (17, 47).

The normalization constant “C” in The Canary Number equation is used to normalize results from Unit to Unit in production stages. This ensures that The Canary Number results from similar tooth clinical situations are consistent regardless of internal variability of detectors, optical design, and electronic variability of each Canary Unit from any production batches.

Raw Canary Numbers can reach a maximum value of approximately 10 000. Therefore, for clinical use and relevance, the raw Canary Number scale is converted to a Normalized Canary Scale of 0–100. In order to provide oral health professionals with a more precise assessment, the Canary Scale is divided into three zones. Zone 1 (0–20) indicates a healthy surface; zone 2 (21–70) may indicate small lesions below the surface or in regions covered with an enamel shell; and zone 3 (71–100) indicates a carious lesion that may require more invasive intervention. The relationship between the raw Canary Number Scale and the Normalized Canary Number scale is shown in Fig. 2. The range of raw Canary Numbers in each zone is determined from Quantum Dental Technologies’ (QDT) Health Canada approved clinical investigational study, QDT-201,^{17,18} through visual inspection of the state of a tooth corresponding to a given Canary Number (intra-oral images). The range of raw Canary Numbers for tooth surfaces that appear healthy is used to define the range of zone 1. Similarly, the ranges of raw Canary Numbers for tooth surfaces that appear to have small lesions and advanced lesions are used to define the ranges of zone 2 and zone 3, respectively. These clinical findings were validated by a parallel investigational extracted tooth study involving sectioning and the examination of each section of tooth by a blinded dental professional.

The generic equation of a straight line is $y = mx + b$, where y is the output value, m is the slope of the line, x is an input value, and b is the y -intercept of the line. As shown in Fig. 2, raw Canary Numbers in logarithmic scale (input) are linearly related to normalized Canary Numbers (output).

Therefore, the following relation can represent the semi-logarithmic plot of Fig. 2:

$$\text{CN}(i) = a(i) \ln(C(i)) + b(i), \quad (2)$$

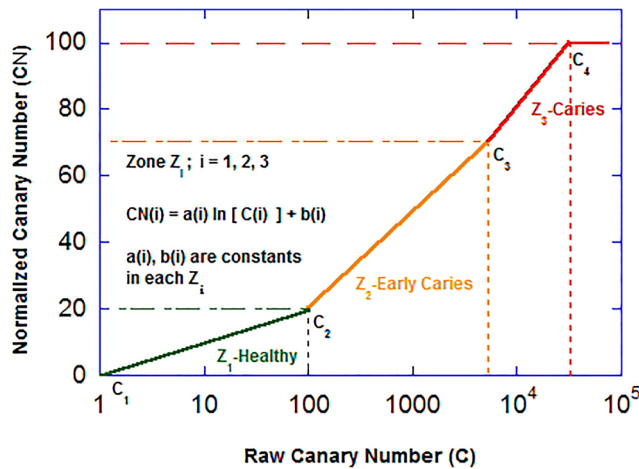


FIG. 2. Normalization of the raw Canary Numbers to a universal 0–100 scale. Normalized Canary Numbers are determined from measured raw Canary Numbers using the equation $CN(i) = a(i) \ln [C(i)] + b(i)$, where $CN(i)$ = Normalized Canary Number (an output value), where $C(i)$ = Raw Canary Number measured by The Canary System (an input value); $i = 1$ (Healthy Zone, Normalized Canary Number 0–20); $i = 2$ (Early Caries Zone, Normalized Canary Number 21–70); and $i = 3$ (Advanced Caries Zone, Normalized Canary Number 71–100). The coefficients “ $a(i)$ ” and “ $b(i)$ ” are the slope and y-intercept of the line in zone (i), respectively. The variables “ $a(i)$ ” and “ $b(i)$ ” are unique to each zone.²⁷ Open-access license: This is an open access article distributed under the terms of the Creative Commons Attribution 4.0 International Public License (CC-BY 4.0).

where $i = 1, 2, 3$ where $i = 1$ [healthy zone (0–20)], $i = 2$ [early caries zone (21–70)], $i = 3$ [advanced caries zone (71–100)], $CN(i)$ = normalized Canary Number, an output value, $C(i)$ = raw Canary Number measured by The Canary System, an input value, $a(i)$ = slope of the line in zone (i), $b(i)$ = y-intercept of the line in Zone (i)

The variables “ $a(i)$ ” and “ $b(i)$ ” are unique to each zone and are determined using the following equations:

$$a(i) = \frac{[CN(i)_{\max} - CN(i)_{\min}]}{\left[\ln \left(\frac{C(i)_{\max}}{C(i)_{\min}} \right) \right]} \quad (3)$$

D. Detecting enamel crack with the PTR-LUM technology

Previous *in vitro* studies using PTR-LUM technology with a 659-nm laser at 5 Hz modulation frequency on a naturally formed radial crack in the thick healthy enamel showed sharp PTR amplitude increases in the crack region. The PTR signal is primarily due to the thermal discontinuity in the cracked region, which occurs along the actual crack configuration and is thus more representative of the actual extent and volume of the crack. However, phase variation from the lateral thermal impedance represented by the crack from healthy teeth would be lost in the noise because only low PTR signals are generated from healthy enamel. (This is why PTR

Phase STD is monitored in The Canary System). Another healthy tooth sample with a slanted natural crack that extended deep into the enamel layer showed that both PTR amplitude and phase detected sharp changes at the crack location. This proof of concept study showed that PTR signals can detect cracks even on healthy enamel depending on the size, orientation, and depth of the crack.^{19,55}

Detecting cracks and caries, especially early caries lesions in enamel, with PTR signals follows similar procedures in both cases. They are defective regions in the crystal structure of the tooth.⁴⁷ With caries, the lesion tends to expand in volume over time, whereas the crack tends to propagate from the tooth surface or from the base of the wall adjacent to a dental restoration. As the crack grows, it may expand in width but it will also expand in length, and this will lead to an area that will trap the laser energy when it is examined with The Canary Systems.

A brief clinical case report was published to highlight the potential to use the PTR-LUM technology for the clinical crack detection.²⁰ However, this manuscript, for the first time, described a longitudinal monitoring of crack development over a few years. It directly demonstrated how PTR -LUM technology could identify and track cracks, that were not seen with radiographs, visually or with an intra-oral camera over time.

III. CLINICAL CASE REPORTS

A. Clinical diagnostic and crack detection

This 61-year-old female has been a patient in a dental group practice of one of the investigators, for over 20 years. During this time, there has been no evidence of bruxism or parafunction. Caries risk had been low and no restorations have been placed or replaced on the right side for over ten years. Four months prior to the examination, the patient began to complain of pain periodically on chewing on the mandibular right posterior area.

Radiographs taken three months prior to the pain occurring did not indicate any caries or cracks on the mandibular first and second molar or on the distal surface of the mandibular right second bicuspid. The maxillary first molar had a large amalgam restoration but there was no pain on hot, cold, percussion, or occlusal loading. The amalgam restorations on the mandibular molar teeth appeared very shallow on bitewing radiographs.

On examination, the pain appeared to be focused on the mesial portion (region A in tooth No. 47, Fig. 3) of the mandibular second molar and distal portion (region B in tooth No. 47, Fig. 3) of the mandibular right first molar. Figure 4 shows the clinical condition of the occlusal surface of the mandibular second molar. There were three shallow amalgams placed in the central area of the occlusal surface over 25 years ago. There were stained grooves on both the mesial and distal marginal ridges. There was a gray shadow on the distal aspect of the distal amalgam. The bitewing radiograph did not indicate that there were caries on the distal aspect (back side) of the tooth and visual examination did not show any open lesion or staining on the distal surface (Fig. 4).

The Canary System was used to scan and examine the occlusal surfaces of the mandibular right second molar. The intra-oral camera image was used to record the location of the various readings. Canary Numbers above 20 indicated that the crystal structure of the tooth was not intact. The Canary examination of this tooth

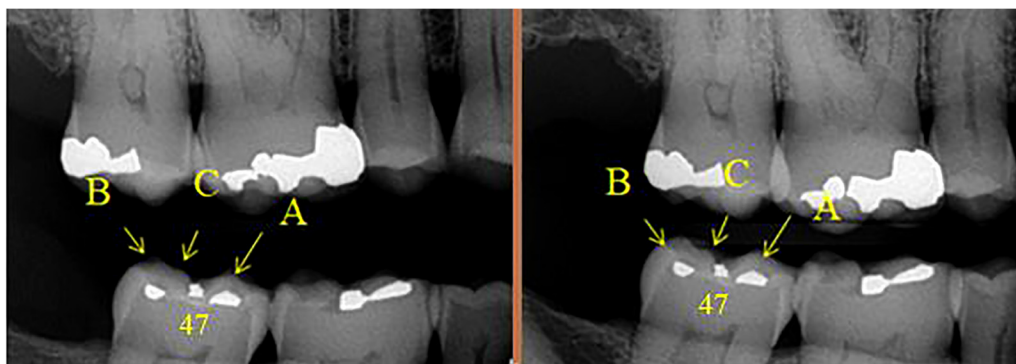


FIG. 3. Bitewing radiographs of the right posterior teeth taken on April 16, 2018 three months before pain occurred.

indicated that the marginal ridges and central pit all have caries and or cracks.

Canary scans are taken on several spots on the enamel surface about a few millimeters away from restoration materials. Studies have been done to validate the ability of The Canary System to detect caries around and beneath the margins of restorations.^{49,57} Canary Number resolutions are ± 5 or less at early carious regions and ± 10 at advanced carious regions of the Canary Scale. Primary source of Canary Number error in clinical scans comes from reproducibility error from spatial variance and angulation of the hand piece than repeatability error from the same sample location. In this report, trained clinicians only took one Canary scan at various regions of interest. There are a number of studies where Canary Number repeatability has been measured and very little variation was found between scans.^{50,53–57}

In Fig. 5, Canary scans taken on a visually intact enamel surface produced Canary No. 14 (in Green Scale). Canary Nos. 0–20 are in

the healthy region as defined in Fig. 2 with related raw Canary Number (69). In Table I, PTR amplitude (6.72 ± 2.32) was low and PTR phase validated that the standard deviation (STD) of PTR phase fluctuations during the Canary Point Scan was very large (26.06 ± 26.96). The phase STD showed that the PTR phase from the thermal response on this scan spot was not locked during the lock-in signal processing calculation of the Canary Number. This PTR Phase STD is a critical parameter to identify healthy enamel spots in the Canary algorithm as described in Eqs. (1)–(3). PTR phase STD will work as a switch to turn ON or OFF LUM Amplitude contribution in Eq. (1). If PTR Phase STD is less than PTR Phase STD set value that was determined from clinical trial results (PTR-phase set value = 15),⁴² then measured LUM Amplitude will take not more than LUM Amplitude set value. LUM Amplitude set value for each Canary Unit (due to variability in optical components and laser source intensity) was determined by instrumental normalization constant C in Eq. (1) using a glassy

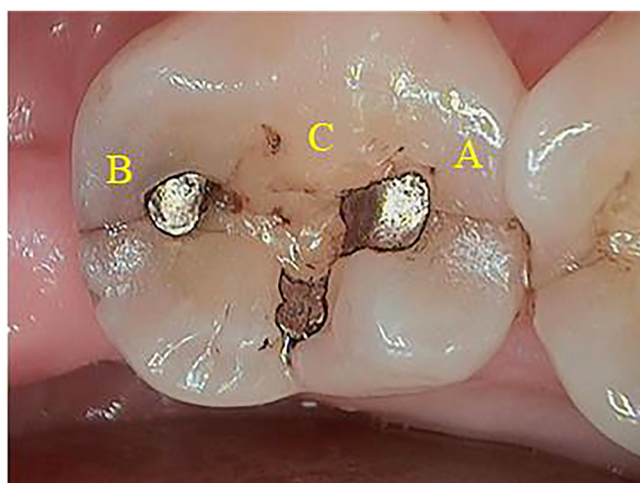


FIG. 4. Occlusal view of the mandibular right second molar (tooth no. 47), November 15, 2018.

Tooth 47 Occlusal
November 15, 2018

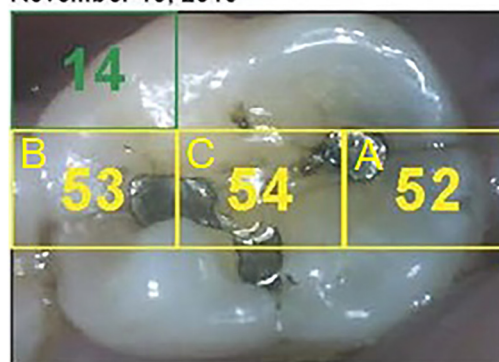


FIG. 5. Canary scan of the occlusal surface of the mandibular right second molar (tooth no. 47). The Canary Scale indicates that there are defects in the crystal structure of the tooth in three locations requiring treatment.

TABLE I. Canary Numbers from The Canary System scan (Fig. 5) and related raw PTR, LUM amplitude, and phase of each point scans are given in this table.

Canary No.	Raw Canary No.	PTR amplitude (AU)	PTR phase (°)	LUM amplitude (AU)	PTR phase (°)
14	69 ± 1.13	6.72 ± 2.32	26.06 ± 26.96	301.95 ± 97.55	179.83 ± 0.17
53	4716 ± 0.13	107.80 ± 7.69	38.05 ± 4.35	102.93	179.51 ± 0.49
54	5178 ± 0.08	134.63 ± 5.38	33.50 ± 2.49	102.93	179.80 ± 0.14
52	4538 ± 0.16	90.15 ± 9.82	43.85 ± 5.71	102.93	179.81 ± 0.11

carbon calibration material. Because of the LUM amplitude limitation, LUM amplitude in Table I for Canary Numbers not in healthy regions recorded a fixed LUM amplitude based on the internal settings of the particular Canary unit. In this clinical situation, if the measured LUM amplitude was less than the fixed LUM amplitude, then measured LUM amplitude would still be allowed without any limitation in the Canary algorithm. White spot lesions generate stronger PTR signals with stronger than healthy LUM amplitude due to the backscattering of light from abnormal enamel crystal structures. This fixed LUM amplitude feature in Canary Number calculation will also improve the sensitivity of white spot early lesion detection in The Canary System. Even though LUM phase contribution in the Canary Number is not significant, LUM phase is also a useful diagnostic parameter to identify biofilms on the scan spot as well as to monitor the hand piece stability during the Canary scans.

Elevated Canary Numbers (52, 53, and 54) in Table I are primarily generated from PTR amplitude and PTR phase. Even though all three Canary Numbers are in a similar range, PTR Amplitude to PTR Phase ratio of 52, 53, and 54 were 2.06, 2.83, and 4.02. Interestingly, Canary Numbers scanned near to the distal (53), mesial (52) crack regions generated similar PTR amplitude/PTR phase ratio of 2.06, 2.83 than Canary Number of the middle region

(54) with 4.02 or healthy region (14) with 0.28 (<1). It could be related to enamel structural integrity of the scanning regions. In this report, these regions of interest are clinically investigated (Fig. 6).

Upon removal of the amalgams on tooth No. 47, cracks were found on the mesial (A—red circle) and distal proximal boxes (B) (Fig. 7). The crack on the distal appeared to be much more extensive (Fig. 7, green circle). There was also some demineralized dentin beneath the amalgam on the distal and some stain from the amalgam (indicated with the green circle). On removal of the amalgam in the central pit, we noted a small crack and leakage around the amalgam margin.

The MOD preparation (mesial, occlusal, and distal filling) was completed and a bonded composite restoration was placed. This restoration has been placed for over 3 years and the patient has had no pain on temperature change or on chewing.

B. Clinical diagnostic examination found additional cracked tooth

1. Canary scans of tooth No. 46 in 2018

We first detected a crack on tooth No. 47 and restored it on November 15, 2018. A bonded composite restoration was placed on tooth No. 47 and when this tooth was prepared, a crack was found on both the mesial and distal areas of the tooth. The Canary scans and images are discussed in the first case report (Sec. III A).

Second case study in this Sec. III B is investigating the history of how the cracks developed initially on tooth No. 47 and then on tooth No. 46. These crack developments clinically validated with supporting high-resolution images and also monitored with the Canary Number results based on PTR-LUM technology.

The patient was seen again on November 27, 2018, since they had cracked the mesial part of the restoration on tooth No. 47 (A—red circle in Fig. 8). At that time, a Canary scan was also taken of the distal surface of tooth No. 46, which was adjacent to the crack. The Canary scan involved scanning from the occlusal or biting surface of the tooth and then scanning between the teeth (interproximal scan). Although there was a stained fissure on the occlusal surface, no cracks were detected with The Canary System.

Periapical radiographs (PR), Fig. 9, nos. 47–46 taken on December 10, 2018 showed no evidence of crack or caries in the interproximal area of No. 46. Tooth No. 46 had worn on the occlusal surface (Fig. 8) but no crack was seen visually, only a stained ridge which could be seen on other molar teeth in this patient.

Canary Numbers from the interproximal area shown in Fig. 8 and background tooth image are combined together to provide a reference tooth image for Canary operators. Tooth image of the interproximal area was first taken with the intra-oral camera in the

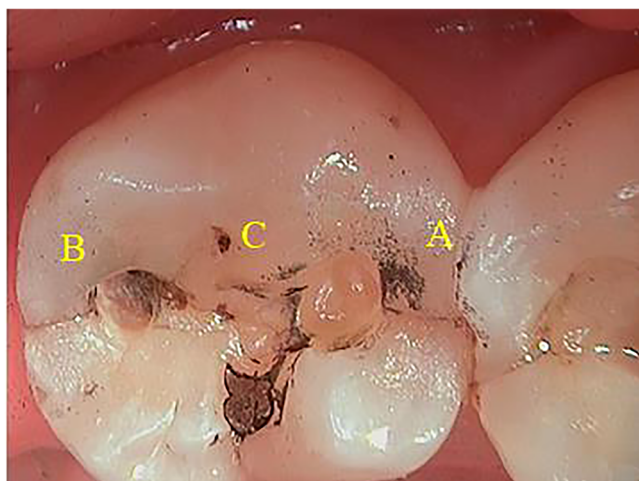


FIG. 6. Initial removal of the amalgam (tooth No. 47) showed cracks on both marginal ridges and some cracks or caries in the central pit. Images taken on November 15, 2018.

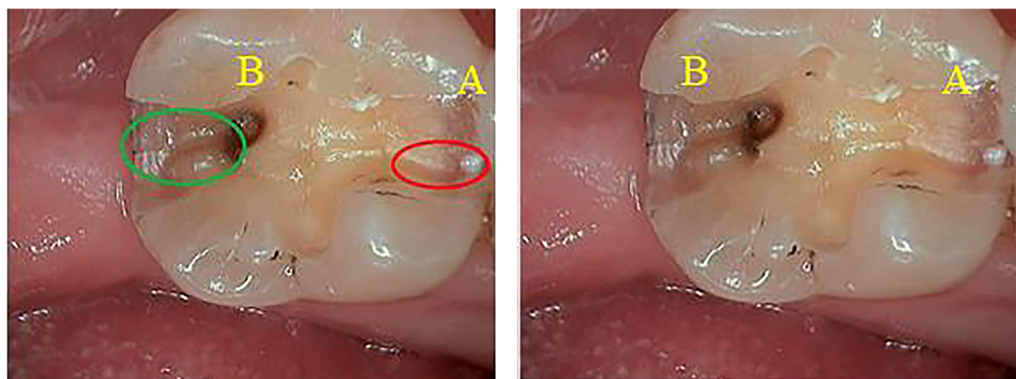


FIG. 7. Image taken after removal of the amalgam (tooth No. 47) and preparation of the proximal boxes. There are still cracks present on the mesial and distal proximal boxes. The circles indicate areas of concern/pathology. Images taken on November 15, 2018.

Canary hand piece then Canary scans were taken on that region. Because of it, Canary Number 23 looks like it was taken outside the interproximal regions. However, all Canary scans were taken on enamel tooth surfaces and not on the gum.

In Fig. 8, Canary scans taken on a visually intact enamel surface produced Canary Number 17 in Green Scale. Canary Numbers 0–20 are in the Healthy region as defined in Fig. 2 with raw Canary Number (200). In Table II, PTR amplitude (8.91 ± 7.67) was low and PTR Phase validated that the standard deviation (STD) of PTR phase fluctuations during the Canary Point Scan was very large (38.92 ± 43.52). Related phase STD showed that PTR phase on this healthy spot was not locked in the Lock-In signal processing calculation (PTR Phase STD >15). Because of this PTR phase STD condition, LUM amplitude in Table II for Canary Numbers (17, 12) showed 205.85 ± 159.45 (not a fixed value) and 102.92 for that

Canary Unit (fixed LUM Amplitude value because corresponding PTR Phase STD was less than 15). Even though both Canary Numbers are in healthy range (<20) during this patient visit, PTR Phase STD (± 9.47) of the Canary Number 12 was locked in the Lock-In signal processing calculation of the scanned data (PTR phase STD >15 for healthy regions).

In this case study, Canary Numbers scanned from this region of interest (ROI) elevated over the years. In the following sections, this scan area was further investigated. Even though PTR Phase results in the ROI showed Canary Number 12, this ROI of tooth No. 46 is an area of concern. That information was not relayed to the dentist because only The Canary Number is provided to the oral health team. The dentist and team only recorded this region as a healthy region at that time. Because, The Canary System with the current regulatory certification from United States Food and Drug

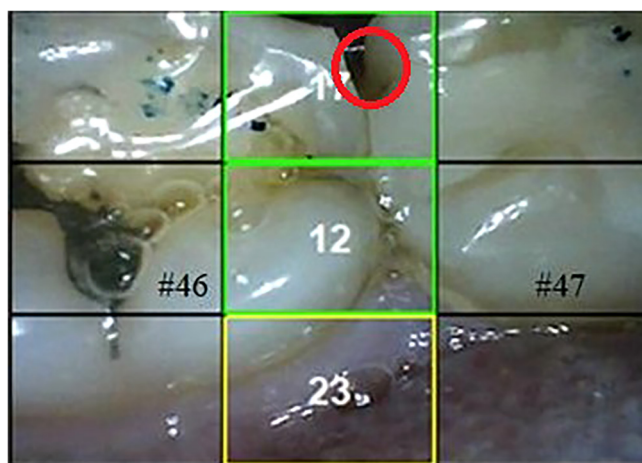


FIG. 8. Canary scan of the distal Interproximal Region of tooth No. 46 Molar. Image taken on November 27, 2018, there was a fracture on the mesial surface of tooth No. 47 indicated with the red circle.



FIG. 9. Bitewing radiographs PA No. 47–46. Image taken on December 10, 2018 showing no evidence of crack or caries in the interproximal area. Tooth No. 46 has wear on the occlusal surface.

TABLE II. Canary Numbers (Fig. 8) from The Canary System on tooth No. 46 from November 27, 2018 and related raw PTR, LUM amplitude, and phase of each point scan are given in this table.

Canary No.	Raw Canary No.	PTR amplitude (AU)	PTR phase (°)	LUM amplitude (AU)	PTR phase (°)
17	200 ± 1.61	8.91 ± 7.67	38.93 ± 43.52	205.85 ± 159.45	179.83 ± 0.65
12	40 ± 2.54	9.38 ± 1.74	3.73 ± 9.47	102.92	179.78 ± 0.12
23	634 ± 0.22	13.49 ± 2.75	40.96 ± 4.06	102.92	179.84 ± 0.16

Administration (FDA) did not have the permission to provide detailed diagnostic information other than the Canary Number output as a diagnostic aid to Dental Health Care providers.

2. Canary scans of tooth No. 46 in 2019

The Canary scan of Occlusal Surface of the 46 Molar was scanned again in April 2019 (5 months after the previous scan as discussed in Sec. III B 1).

Figure 10 shows the Canary Scan results taken on the occlusal surface of tooth No. 46.

In Fig. 10, all Canary scanned results taken on the occlusal surface of tooth No. 46 were in healthy regions. However Table III shows that The Canary scan taken on distal area with Canary Number 18 on tooth No.46, the same region discussed in the previous section (Canary Number 12 in Table II), again showed that the PTR Phase (9.38 ± 10.98) was locked in Lock-In results (PTR Phase STD <15). All other Canary scanned spots revealed healthy Canary Numbers with PTR Phase STD were larger than the PTR phase STD for the healthy regions (PTR Phase STD >15).

In this case study, Canary Numbers scanned from this area are increasing over the time. In the following sections, this scan area was further investigated with clinical evidence. Even though this PTR phase results (9.38 ± 10.98 in Table III) taken 5 months

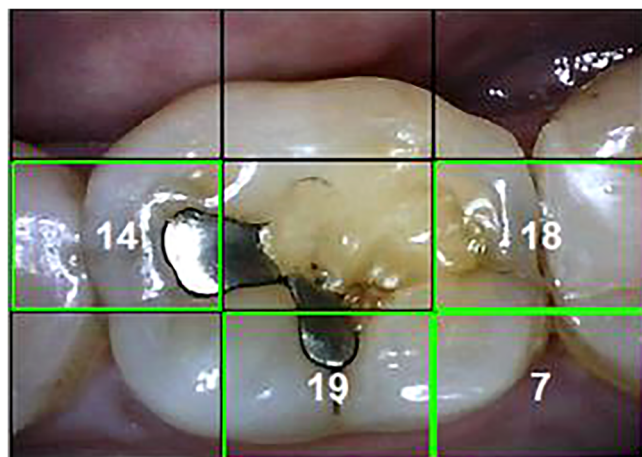


FIG. 10. Canary scan of the Occlusal Surface of the 46 Molar (April 2019). The adjacent surface of tooth No. 47 which was cracked in November 27, 2018 is intact.

after the first Canary scan, PTR phase STD results showed again that this area with Canary Number 18 could be an area of concern. That information was not relayed to the dentist since The Canary System only provided The Canary Number and not the individual PTR and LUM results. Canary operators only recorded this region as a healthy spot at this time.

Without knowing the elevating PTR Phase results hidden in The Canary Number in healthy region [Canary Number changed from 12 to 18 and still in healthy region (<20) and dentist continued to monitor tooth No. 46 for evidence of a crack]. A bite splint was fabricated and given to the patient in June 2019 to cover all the mandibular (lower teeth) and protect them from grinding when the patient was sleeping (Figs. 11–14).

3. Canary scans of tooth no. 46 in 2020

Since the patient was asymptomatic and there were issues with appointments during COVID-19 no Canary scans were done in 2020. Repeat scans and radiographs were taken and in March 2021, a crack was found on tooth No. 46 and an MOD composite restoration was placed.

4. Canary scans of tooth No. 46 in 2021

Occlusal surface of the tooth No. 46 scanned with The Canary System at that time and elevated Canary Numbers were found (Fig. 15) on the distal area. The Canary Numbers 27 and 21 were recorded from scans done on through the side contact or interproximal regions.

In Fig. 15, Canary scanned results taken on the mesial area of tooth No.46 was in the health region (Canary Number 20). Similar to Canary scan taken on distal area of tooth No. 46 in the previous sections, PTR phase (28.80 ± 4.99) was locked in Lock-In results. Even though the enamel surface of this mesial area of tooth No.46 looked healthy, PTR-phase and its STD showed this area is a concern.

Canary Numbers (56, 27, and 21) of the distal region of tooth No.46 that have been monitored in previous sections for years are now elevated with The Canary Number on the occlusal surface over the marginal ridge being significantly elevated to Canary Number 56.

The Canary Numbers of the enamel structure of the middle of the distal area that showed healthy regions in the previous sections with locked PTR-phase STD (9.38 ± 10.98 in Table III) was greatly affected. Canary Numbers recorded in this area with 12 in 2018 (Table II) and 18 in 2019 (Table III) was elevated to 56 in 2021 (Table IV).

TABLE III. Canary Numbers (Fig. 10) from The Canary System and related raw PTR, LUM amplitude, and phase of each point scans taken in April 2019 are given in table.

Canary No.	Raw Canary No.	PTR amplitude (AU)	PTR phase (°)	LUM amplitude (AU)	PTR phase (°)
18	246 ± 1.20	21.85 ± 5.94	9.38 ± 10.98	16.7	179.65 ± 0.16
19	350 ± 3.05	98.09 ± 92.29	10.34 ± 29.80	58.78 ± 20.56	179.57 ± 0.92
7	10 ± 4.13	2.08 ± 3.18	13.74 ± 50.67	58.78 ± 20.56	179.86 ± 0.45
14	89 ± 1.37	6.07 ± 4.96	42.52 ± 44.32	58.78 ± 20.56	179.10 ± 0.33



FIG. 11. Occlusal view of tooth No. 46 showing stained groove (inside the black circle) on the distal marginal ridge (Image taken on April 30, 2019).

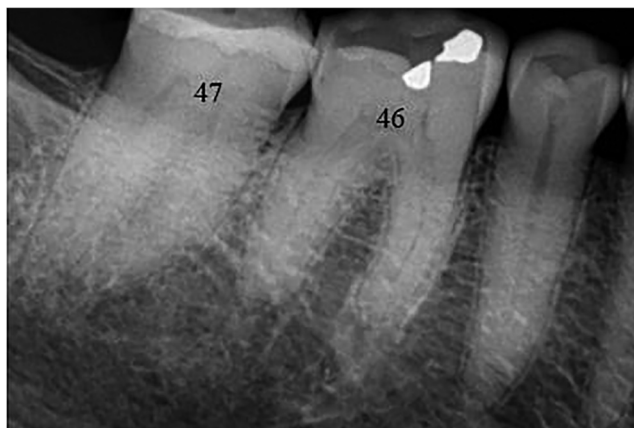


FIG. 13. PA of nos. 47–46 shows no issues with the distal margin of tooth No. 46. Image taken on November 18, 2019.



FIG. 12. Shows the occlusal view No. 47–45. Image taken on April 30, 2019. Tooth No. 46 has wear (inside the black circle) on the distal surface and no visible cracks.

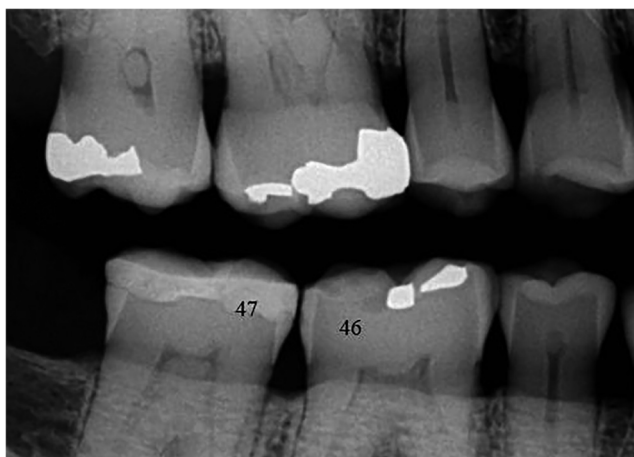


FIG. 14. Bitewing right side showing no crack on distal marginal ridge No. 46. Image taken on July 20, 2020.

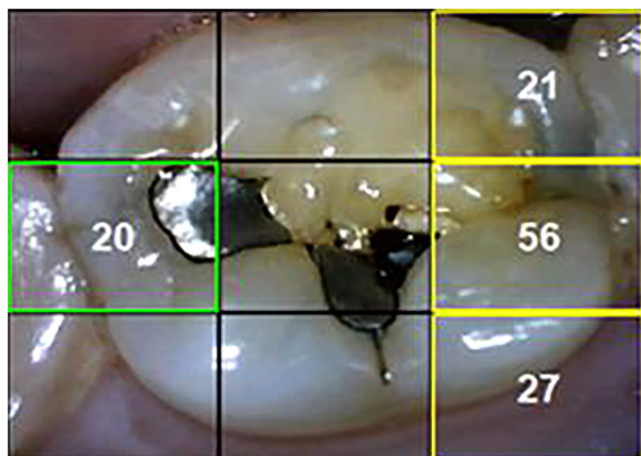


FIG. 15. March 4, 2021 Canary scan taken on tooth No. 46 indicated that there was a crack on the distal marginal ridge adjacent to tooth No. 47, the tooth with the original crack.

Table V shows the changes in the Canary Number on the distal area of the region of interests over 3 years of monitoring time. The Canary Number was increasing over time because PTR amplitude and PTR phase are directly proportional as well as LUM Amplitude and LUM Phase are indirectly proportional to the raw Canary Number [Eq. (1)]. Then raw Canary Number is normalized to Canary Number in 0–100 scale [Eqs. (2) and (3) with related boundary values from clinical trial results].

Table VI shows that the Canary Numbers of cracks described in Table I (tooth No. 47) and Table IV (tooth No. 46) of open and hidden cracks at different depths. Even though the Canary operator only recorded similar Canary Numbers (52, 56) from these teeth, PTR, LUM amplitude and phase results from those scanned spots had more diagnostic information on the status of the tooth structure that could be validated with images of the tooth captured after the tooth was prepared for a restoration.

Clinical evidence showed that tooth No. 47 had a deep crack with opening on the surface and tooth No. 46 had a hidden crack with caries (darker regions in middle of the distal area in Fig. 16) underneath intact enamel. Because of this clinical situation, elevated PTR Amplitude and PTR Phase results were recorded in the crack region of tooth No.47 (Canary Number 52). Even though Canary Number (56) on tooth No. 46 was in a similar range, related PTR amplitude and PTR phase were not as high as open

cracks in tooth No. 47. This is because thin healthy enamel was still attenuating the thermal response from the deeper carious and crack regions. Images of these distal regions further validating that no visible stains on that region and hence the drop in the LUM Amplitude and LUM phase was primarily contributed to the elevated Canary Number (56) on tooth No. 46. As PTR phase is a sensitivity parameter to identify non-healthy enamel regions, tooth No. 46 results in this clinical situation showed that LUM phase is also an important parameter to identify hidden defects under thin healthy enamel (Figs. 17 and 18).

IV. DISCUSSION

Detecting cracks is a clinical challenge.²⁸ At times, the symptoms may not be indicative of the presence of a crack.² As we have seen in this case report, bitewing radiographs may not be able to image small micro-fractures. Clinicians then need to find caries detection devices that image, measure and monitor defects, cracks and caries.

Visual examination may detect surface staining. Probing with an explorer may find pits and fissures but these might not be indicative of a crack or caries. Studies indicate that classical use of sharp explorers may produce irreversible traumatic defects in demineralized areas in occlusal fissures favoring conditions for isolated lesion progression.^{16,29}

Fluorescence is one method that is being used for caries detection. Fluorescence is simply the emission of light from an object that has absorbed light at a specific wavelength. This is the core technology in SOPROLIFE (Acteon), Spectra (Air Techniques), and DIAGNODENT (KaVo).³⁰ These devices produce glow from the tooth surface when an LED or laser light is shone on the tooth. The research literature indicates that the glow is from one or more of the following whether or not caries is present:^{31–37} bacterial porphyrins (bacterial breakdown product),^{38,39} stain, tartar, food debris.

Another problem with fluorescence is that it does not penetrate beneath the tooth surface due to scattering of light from stain, plaque, organic deposits and surface features such as pits and fissures.^{42,43} Studies have also demonstrated poor correlation between DIAGNODent and other fluorescence devices readings with caries lesion depth.^{16,40,41,44–46} This indicates that fluorescence based devices may not be able to detect cracks in teeth. When a crack occurs near a restoration then the fluorescence or glow from the restoration may impede the ability of the device to detect any information from the enamel surface.

These case studies results clinically validated that carious lesions modify the thermal properties (PTR) and glow (LUM) from

TABLE IV. Canary Numbers (Fig. 15) from The Canary System and related raw PTR, LUM amplitude, and phase of each point scans are given in table.

Canary No.	Raw Canary No.	PTR amplitude (AU)	PTR phase (°)	LUM amplitude (AU)	PTR Phase (°)
20	477 ± 0.24	16.13 ± 2.72	28.80 ± 4.99	30.38	178.75 ± 1.35
56	5660 ± 0.40	31.50 ± 6.51	19.39 ± 3.09	3.76 ± 1.15	159.86 ± 4.96
27	822 ± 0.43	7.71 ± 1.04	18.48 ± 5.03	5.85 ± 1.82	165.35 ± 3.93
21	546 ± 0.99	16.27 ± 4.41	21.39 ± 20.25	20.60 ± 2.11	165.38 ± 5.75

TABLE V. Summary of the changes in the Canary Numbers of distal occlusal area of tooth No. 46 in 2018, 2019, and 2021 with related raw PTR, LUM amplitude, and phase of each point scans are given in table.

Date	Canary No.	Raw Canary No.	PTR amplitude (AU)	PTR phase (°)	LUM amplitude (AU)	PTR phase (°)
2018	12	40 ± 2.54	9.38 ± 1.74	3.73 ± 9.47	102.92	179.78 ± 0.12
2019	18	246 ± 1.20	21.85 ± 5.94	9.38 ± 10.98	16.7	179.65 ± 0.16
2021	56	5660 ± 0.40	31.50 ± 6.51	19.39 ± 3.09	3.76 ± 1.15	159.86 ± 4.96

the healthy teeth. As a lesion grows, there is a corresponding change in the signal as the heat is confined to the region with crystalline disintegration (dental caries); PTR increases and LUM decreases. As remineralization progresses and enamel prisms begin to reform their structure, the thermal and luminescence properties begin to revert back in the direction of healthy teeth.^{42–47} However, in this case report, remineralization results with clinical evidence with PTR-LUM technology was not discussed.

This case study results showed that the Canary Number (ranging from 0 to 100) is created from an algorithm combining the PTR and LUM readings and is directly linked to the status of the enamel or root surface crystal structure.^{47,48} A Canary Number of less than 20 indicates a healthy tooth surface. Any Canary Number above 20 indicates an early or advanced defect in the tooth structure.⁴⁹ In this clinical situation, The Canary Numbers were above 50, indicating large cracks or extensive cracks along the marginal ridges and caries in the central pit. These cracks were found upon preparation of the tooth for the restoration and not seen on radiographs. The cracks are also indicative that the patient was clenching and grinding. The dentist fabricated and provided the patient with a night splint and continued to monitor the patient for bruxism and parafunction and other TMD issues. This bite splint was placed in June 2019 after the first crack was detected in November 2018.

In order to detail the scientific evidence behind the PTR-LUM technology in clinical dentistry for crack and defect detection, PTR technology based crack detection imaging research for industrial engineering applications by Mandelis' group is highlighted in this section.^{51,52} Since PTR-LUM technology used for crack detection on teeth is a Point Scan system, relating the same application with 2D PTR imaging results obtained from same Lock-In image processing principles for detecting cracks on Pre-sintered ("green") compressed metal powder components may help to visualize the results from the PTR-LUM technology discussed in this work.⁵¹

In this case study, hidden crack formation caused by biomechanical stress/tooth grinding caused the creation and expansion of the crack. The findings were validated during the restorative clinical procedures. Studies have shown that the PTR Phase changes would be discontinuous within crack regions.^{51,52} This effect was also validated with Phase images generated from lock-in signal processing algorithms in independent reports.⁵¹ In a recent *in vitro* study, Mandelis' group also showed the capability of the PTR technology for detecting cracks on enamel and validated with micro-computed tomography (μ CT).⁴⁷

The Physics of monitoring cracks on enamel crystal structures with Amplitude and Phase responses of the PTR signal in The Canary System is the same as the Physics of detecting cracks on Pre-sintered compressed metal powder components with lock-in signal processing. However, the existence of highly scattering and depth absorbing dental tissue generates thermal signals that are quite different from those in engineering materials like automotive parts. One disadvantage of visualizing the crack on tooth structure is due to the fact that The Canary System is a Point Scan System. It can measure an area of 1.5 mm. in diameter up to 5.0 mm. in depth. Current dental market cannot afford PTR-LUM based imaging systems to explicitly visualize 2D, 3D crack and carious regions even though proof of concept studies of such applications have already been published by Mandelis' group.⁴⁷

This case study report used The Canary System Point Scan to detect cracks in teeth. It initially detected a crack on a back molar and the dentist continued to monitor the adjacent tooth since there were concerns that the patient was grinding or clenching during the day or while asleep. The adjacent molar developed a crack with symptoms 3 years later which was detected by The Canary System. The cracks were not seen with radiographs or visually. The initial crack was detected after the patient reported symptoms on chewing. The presence of the cracks was validated with intra-oral camera images taken during the placement of the bonded

TABLE VI. Canary Numbers of cracks shown in Table I (tooth No. 47) and Table IV (tooth No. 46) of open and hidden cracks at different depths are shown with related raw PTR, LUM amplitude, and phase results in table.

Tooth No. and date	Canary No.	Raw Canary No.	PTR amplitude (AU)	PTR phase (°)	LUM amplitude (AU)	PTR phase (°)
Tooth No. 47 November 2018	52	4538 ± 0.16	90.15 ± 9.82	43.85 ± 5.71	102.93	179.81 ± 0.11
Tooth No. 46 March 2021	56	5660 ± 0.40	31.50 ± 6.51	19.39 ± 3.09	3.76 ± 1.15	159.86 ± 4.96

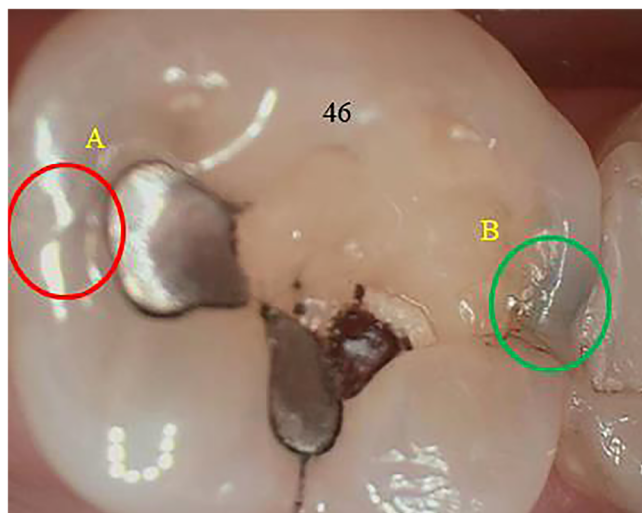


FIG. 16. Restoration of tooth No. 46. Image taken on March 4, 2021. Stained distal marginal ridge and caries on mesial under amalgam.

composite filling. Since the clinical PTR-LUM based Point Scan System (The Canary System) can only be used as a caries detection aid, its information becomes a critical part of developing a diagnosis and treatment plan. The Canary System can detect and monitor defects in tooth structure including caries, cracks, and erosion of the tooth surface, detection of caries around restorations/fillings, and re-hardening of early areas of caries.

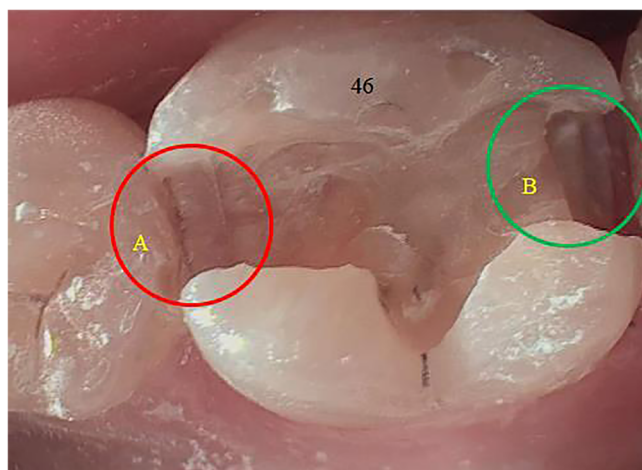


FIG. 17. Preparation on tooth No. 46 shows crack on distal box and distal area (B—green circle). Figure also shows stain and caries on the mesial area of tooth No. 46 (A—red circle).

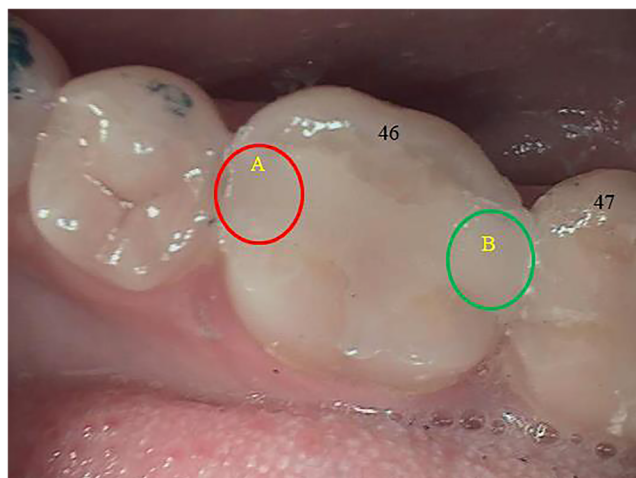


FIG. 18. Shows completed restoration on tooth No. 46 with a bonded composite resin. The mesial surface of tooth No. 47 is visible showing it is intact with no signs of wear or marginal openings around the composite restoration.

V. CONCLUSIONS

Detecting cracks in teeth is a clinical challenge. A good clinical history and an accurate caries detection system such as The Canary System based on PTR-LUM technology can provide the clinician with the tools needed to detect cracks and caries. Once found, the cracks can be treated with the placement of direct restorations or full coverage restorations. One also needs to assess the cause of the cracks and how best to prevent them from occurring in the future. The Canary System will allow oral health providers to not only detect cracks but to monitor teeth for changes and cracks over time.

AUTHOR DECLARATIONS

Conflict of Interest

Dr. Stephen Abrams and Dr. Andreas Mandelis are the co-founders of Quantum Dental Technologies, which has developed The Canary System. Dr. Stephen Abrams has not received any compensation for this article. Dr. Mandelis was not consulted or involved in the design and the writing of this article. Koneswaran Sivagurunathan was the VP Product Development at Quantum Dental Technologies (2007–2021). He has not received any compensation for this article.

DATA AVAILABILITY

The clinical raw data that support the findings of this study are provided in [Tables I–VI](#) and further data from similar clinical situations are available from the corresponding author upon reasonable request.

REFERENCES

- C. E. Cameron, “Cracked-tooth syndrome,” *JADA* **68**, 405–411 (1964).

- ²S. Banerji, S. B. Mehta, and B. J. Millar, "Cracked tooth syndrome. Part 1: Aetiology and diagnosis," *Br. Dent. J.* **208**(10), 459–463 (2010).
- ³S. Hasan, K. Singh, and N. Salati, "Cracked tooth syndrome: Overview of literature," *Int. J. Appl. Basic Med. Res.* **5**, 164–168 (2015).
- ⁴C. E. Cameron, "The cracked tooth syndrome: Additional findings," *JADA* **93**, 971–975 (1976).
- ⁵J. D. Bader, J. A. Martin, and D. A. Shugars, "Preliminary estimates of the incidence and consequences of tooth fracture," *JADA* **126**, 1650–1654 (1995).
- ⁶H. Rosen, "Cracked tooth syndrome," *J. Prosthet. Dent.* **47**, 36–43 (1982).
- ⁷J. D. Bader, J. A. Martin, and D. A. Shugars, "Incidence rates for complete cusp fracture," *Community Dent. Oral Epidemiol.* **29**, 346–353 (2001).
- ⁸B. V. Braly and E. H. Maxwell, "Potential for tooth fracture in restorative dentistry," *J. Prosthet. Dent.* **45**, 411–414 (1981).
- ⁹M. E. Gher, Jr., R. M. Dunlap, M. H. Anderson, and L. V. Kuhl, "Clinical survey of fractured teeth," *JADA* **114**, 174–187 (1987).
- ¹⁰C. I. Homewood, "Cracked tooth syndrome—Incidence, clinical findings and treatment," *Aust. Dent. J.* **43**, 217–222 (1998).
- ¹¹S. Ratcliff, I. M. Becker, and L. Quinn, "Type and incidence of cracks in posterior teeth," *J. Prosthet. Dent.* **86**, 168–172 (2001).
- ¹²D.-G. Seo Y. Young-Ah *et al.*, "Analysis of factors associated with cracked teeth," *JOE* **38**(3), 288–292 (2012).
- ¹³B. D. Roh and Y. E. Lee, "Analysis of 154 cases of teeth with cracks," *Dent. Traumatol.* **22**, 118–123 (2006).
- ¹⁴Institute AHP, COVID 19: Economic Impact on Practices Week of February 15 American Dental Association 2021:130.
- ¹⁵A. Emodi-Perlman, I. Eli, J. Smardz *et al.*, "Temporomandibular disorders and bruxism outbreak as a possible factor of orofacial pain worsening during the COVID-19 pandemic-concomitant research in two countries," *J. Clin. Med.* **9**(10), 3250 (2020).
- ¹⁶K. Ekstrand, V. Qvist, and A. Thylstrup, "Light microscopic study of the effect of probing in occlusal surfaces," *Caries Res.* **21**, 368–374 (1987).
- ¹⁷K. Sivagurunathan, S. H. Abrams, J. Garcia, A. Mandelis, B. T. Amaechi, Y. Finer, W. M. P. Hellen, and G. Elman, "Using PTR-LUM ('The Canary System') for *in vivo* detection of dental caries: Clinical trial results," *Caries Res.* **44**, 171–247 (2010).
- ¹⁸J. D. Silvertown, S. H. Sivagurunathan, K. S. Kennedy, J. Jeon, J. Mandelis, A. Hellen, A. Hellen, W. Elman, G. Ehrlich, R. Chouljian, R. Finer, Y. Amaechi, and B. T. "Multi-centre clinical evaluation of photothermal radiometry and luminescence correlated with international benchmarks for caries detection," *Open Dent. J.* **11**, 636–647 (2017).
- ¹⁹R. J. Jeon, C. Han, A. Mandelis, V. Sanchez, and S. H. Abrams, "Diagnosis of pit and fissure caries using frequency-domain infrared photothermal radiometry and modulated laser luminescence," *Caries Res.* **38**(6), 497–513 (2004).
- ²⁰S. H. Abrams, "Improving the ways to detect cracks in teeth," *Dent. Today* **32**(7), 104–107 (2013).
- ²¹R. J. Jeon, A. Mandelis, V. Sanchez, and S. H. Abrams, "Noninvasive, noncontacting frequency-domain photothermal radiometry and luminescence depth profilometry of carious and artificial subsurface lesions in human teeth," *J. Biomed. Opt.* **9**(4), 804–819 (2004).
- ²²L. Nicolaidis, A. Mandelis, and S. H. Abrams, "Novel dental dynamic depth profilometric imaging using simultaneous frequency-domain infrared photothermal radiometry and laser luminescence," *J. Biomed. Opt.* **5**(1), 31–39 (2000).
- ²³L. Nicolaidis, C. Feng, A. Mandelis, and S. H. Abrams, "Quantitative dental measurements by use of simultaneous frequency-domain laser infrared radiometry and luminescence," *Appl. Opt.* **41**(4), 768–777 (2002).
- ²⁴A. Matvienko, A. Mandelis, R. J. Jeon, and S. H. Abrams, "Theoretical analysis of coupled diffuse-photon-density and thermal-wave field depth profiles photothermally generated in layered turbid dental structures," *J. Appl. Phys.* **105**, 102022 (2009).
- ²⁵A. Hellen, A. Matvienko, A. Mandelis, Y. Finer, and B. T. Amaechi, "Optothermophysical properties of demineralized human dental enamel determined using photothermally generated diffuse photon density and thermal wave fields," *Appl. Opt.* **49**(36), 6938–6951 (2010).
- ²⁶J. Kim, A. Mandelis, S. H. Abrams, J. T. Vu, and B. T. Amaechi, "In-vitro detection of artificial caries on vertical dental cavity walls using infrared photothermal radiometry and modulated luminescence," *J. Biomed. Opt.* **17**(12), 127001 (2012).
- ²⁷S. H. Abrams, K. S. Sivagurunathan, J. D. Silvertown, B. Wong, A. Hellen, A. Mandelis, W. M. P. Hellen, G. I. Elman, S. K. Mathew, P. K. Mensinkai, and B. T. Amaechi, "Correlation with caries lesion depth of The Canary System, DIAGNOdent and ICDAS II," *Open Dent. J.* **11**, 679–689 (2017).
- ²⁸S. Abrams, "Improving the way to detect cracks in teeth," *Dent. Today* **32**(7), 104–106 (2013).
- ²⁹N. B. Pitts, "Diagnostic tools and measurements- impact on appropriate care," *Community Dent. Oral Epidemiol.* **25**, 24–35 (1997).
- ³⁰P. Rechmann and J. D. Featherstone, "Caries detection using light-based diagnostic tools," *Compend. Contin. Educ. Dent.* **33**(88), 582–593 (2012).
- ³¹A. I. S. Lussi, N. Pitts, C. Longbottom, and E. Reich, "Performance and reproducibility of a laser fluorescence system for detection of occlusal caries *in vitro*," *Caries Res.* **33**(4), 261–266 (1999).
- ³²A. H. R. Lussi and R. Paulus, "DIAGNOdent: An optical method for caries detection," *J. Dent. Res.* **83**, C80–C83 (2004).
- ³³E. H. v. d. V. M. Verdonchot, "Lasers in dentistry 2. Diagnosis of dental caries with lasers," *Ned. Tijdschr. Tandheelkd.* **109**(4), 122–126 (2002).
- ³⁴K. F. G. König and R. Hibst, "Laser-induced autofluorescence spectroscopy of dental caries," *Cell Mol. Biol. (Noisy-le-grand)* **44**(8), 1293–300 (1998).
- ³⁵H. M. P. A. Alwas-Danowska, S. Suliborski, and E. H. Verdonchot, "Reliability and validity issues of laser fluorescence measurements in occlusal caries diagnosis," *J. Dent.* **30**(4), 129–134 (2002).
- ³⁶Á. Ástvaldsdóttir, S. Tranæus, L. Karlsson, and W. Peter Holbrook, "DIAGNOdent measurements of cultures of selected oral bacteria and demineralized enamel," *Acta Odontol. Scand.* **68**(3), 148–153 (2010).
- ³⁷R. W. V. Liang, M. Marcus, P. Burns, and P. McLaughlin, "Multimodal imaging system for dental caries detection," in *Proceedings of SPIE Lasers in Dentistry* (SPIE, 2007), p. XIII (64502).
- ³⁸A. G. J. Hall, "A review of potential new diagnostic modalities for caries lesions," *J. Dent. Res.* **83**, C89–94 (2004).
- ³⁹M. A. B. J. Khalife, J. B. Dennison, P. Yaman, and J. C. Hamilton, "In vivo evaluation of DIAGNOdent for the quantification of occlusal dental caries," *Oper. Dent.* **34**(2), 136–14 (2009).
- ⁴⁰A. R. D. Jablonski-Momeni, S. Rolfsen, R. Stoll, M. Heinz-Gutenbrunner, V. Stachniss, and K. Pieper, "Performance of laser fluorescence at tooth surface and histological section," *Lasers Med. Sci.* **26**(2), 171–178 (2011).
- ⁴¹T. F. Novaes, C. M. Moriyama, M. S. De Benedetto *et al.*, "Performance of fluorescence-based methods for detecting and quantifying smooth-surface caries lesions in primary teeth: An *in vitro* study," *Int. J. Paediatr. Dent.* **26**(1), 13–19 (2016).
- ⁴²R. J. Jeon, T. D. T. Phan, A. Wu, G. Kulkarni, S. H. Abrams, and A. Mandelis, "Photothermal radiometric quantitative detection of the different degrees of demineralization of dental enamel by acid etching," in *Proceedings of 13th International Conference on Photoacoustic & Photothermal Phenomena, July 5–8 2004* [J. Phys. IV France **125**, 721–723 (2005)].
- ⁴³R. J. Jeon, A. Matvienko, A. Mandelis, S. H. Abrams, B. T. Amaechi, and G. Kulkarni, "Detection of interproximal demineralized lesions on human teeth *in vitro* using frequency-domain infrared photothermal radiometry and modulated luminescence," *J. Biomed. Opt.* **12**(3), 034028 (2007).
- ⁴⁴A. Matvienko, R. J. Jeon, A. Mandelis, S. H. Abrams, and B. T. Amaechi, "Photothermal detection of incipient dental caries: Experiment and modeling," *Proc. SPIE* **66759J**, 67590J-1–67590J-10 (2007).
- ⁴⁵R. J. Jeon, A. Hellen, A. Matvienko, A. Mandelis, S. H. Abrams, and B. T. Amaechi, "Experimental investigation of demineralization and remineralization of human teeth using infrared photothermal radiometry and modulated luminescence," in *Proceedings of SPIE, SPIE BiOS, San Jose, January 2008* (SPIE, 2008), Vol. 6856, p. 68560B.
- ⁴⁶A. Matvienko, A. Mandelis, and S. H. Abrams, "Robust multi-parameter evaluation method of optical and thermal properties of a layered tissue structure using photothermal radiometry," *Appl. Opt.* **48**(17), 3193–3204 (2009).

- ⁴⁷S. Roointan, P. Tavakolian, K. S. Sivagurunathan *et al.*, “3D dental subsurface imaging using enhanced truncated correlation-photothermal coherence tomography,” *Sci. Rep.* **9**, 16788 (2019).
- ⁴⁸J. Garcia, A. Mandelis, S. H. Abrams, and A. Matvienko, “Photothermal radiometry and modulated luminescence: Application to dental caries detection,” in *Handbook of Biophotonics, Photonics for Health Care*, edited by J. Popp, V. V. Tuchin, A. Chiou, and S. H. Heinemann (Wiley-VCH, 2011), Vol. 2, Chap. 71, p. 1047.
- ⁴⁹T. Abrams, S. Abrams, K. Sivagurunathan *et al.*, “Detection of caries around resin-modified glass ionomer and compomer restorations using four different modalities *in vitro*,” *Dent. J.* **6**(3), 47 (2018).
- ⁵⁰B. A. T. Wong, K. Sivagurunathan, J. D. Silvertown, L. O. Okoye, S. H. Abrams, and B. T. Amaechi, “Evaluation of inter- and intra-examiner reproducibility of The Canary System,” *J. Dent. Res.* **94**, 1479 (2015).
- ⁵¹K. Sebastian, A. Melnikov, K. Sivagurunathan, X. Guo, X. Wang, and A. Mandelis, “Non-destructive lock-in thermography of green powder metallurgy component inhomogeneities: A predictive imaging method for manufactured component flaw prevention,” *NDT&E Int.* **127**, 102603 (2022).
- ⁵²A. Melnikov, K. Sivagurunathan, X. Guo, J. Tolev, A. Mandelis, K. Ly, and R. Lawcock, “Non-destructive thermal-wave-radar imaging of manufactured green powder metallurgy compact flaws (cracks),” *NDT&E Int.* **86**, 140–152 (2017).
- ⁵³A. F. Dayo, B. T. Amaechi, M. Noujeim *et al.*, “Comparison of photothermal radiometry and modulated luminescence, intraoral radiography, and cone beam computed tomography for detection of natural caries under restorations,” *Oral Surg. Oral Med. Oral Pathol. Oral Radiol.* **129**(5), 539–548 (2020).
- ⁵⁴J. Jan, W. Z. Wan Bakar, S. M. Mathews, E. Uzamere, L. O. Okoye, and T. Bennett, “Amaechi. Clinical trial of The Canary System for proximal caries detection: A comparative study,” *J. Biomed. Opt.* **26**(4), 046004 (2021).
- ⁵⁵J. Jan, W. Z. W. Bakar, S. M. Mathews, E. Uzamere, O. L. Okoye, and T. B. Amaechi, “Clinical trial of The Canary System for proximal caries detection: A comparative study,” *Curr. J. Appl. Sci. Technol.* **40**(35), 38–50 (2021).
- ⁵⁶R. J. Jeon, A. Mandelis, and S. H. Abrams, “Depth profilometric case studies in caries diagnostics of human teeth using modulated laser radiometry and luminescence,” *Rev. Sci. Instrum.* **74**, 380–383 (2003).
- ⁵⁷T. E. Abrams, S. H. Abrams, K. S. Sivagurunathan, J. D. Silvertown, W. M. P. Hellen, G. I. Elman, and B. T. Amaechi, “*In vitro* detection of caries around amalgam restorations using four different modalities,” *Open Dent. J.* **11**, 609–620 (2017).